

Soft x-ray absorption and photoemission spectroscopy study of superoxide KO_2

J.-S. Kang,* D. H. Kim, and J. H. Hwang

Department of Physics, The Catholic University of Korea, Bucheon 420-743, Korea

J. Baik and H. J. Shin

Pohang Accelerator Laboratory (PAL), POSTECH, Pohang 790-784, Korea

Minjae Kim, Y. H. Jeong, and B. I. Min

Department of Physics, POSTECH, Pohang 790-784, Korea

(Received 20 July 2010; revised manuscript received 24 September 2010; published 22 November 2010)

The electronic structure of superoxide KO_2 was investigated by employing soft x-ray absorption spectroscopy (XAS) and core-level photoemission spectroscopy (PES). The clean and single component was observed in both the O $1s$ and K $2p$ core-level PES spectra of KO_2 , which confirms the good quality of the KO_2 sample employed in this work. The measured O $1s$ XAS spectrum was compared with the calculated density of states (DOSs), obtained from the first-principles electronic-structure calculations that include both the spin-orbit (SO) effect and the on-site Coulomb interaction (U) between O $2p$ electrons. In the O $1s$ XAS, both the unoccupied O $2p$ antibonding π_g and σ_u states are identified. It is found that the unoccupied states, observed in the O $1s$ XAS, agree reasonably well with the calculated DOSs, which suggests the importance of the SO and U effects for KO_2 having the high-symmetry tetragonal structure.

DOI: [10.1103/PhysRevB.82.193102](https://doi.org/10.1103/PhysRevB.82.193102)

PACS number(s): 78.70.Dm, 79.60.-i, 75.47.Lx, 71.70.Ej

I. INTRODUCTION

AO_2 -type alkali superoxides ($A=\text{Na}, \text{K}, \text{Rb}, \text{Cs}$), which can be regarded as ionic molecular crystals, are very interesting since they exhibit magnetism even though they do not contain the partially filled d or f electrons.¹ In AO_2 , one alkali-metal atom provides one electron to an oxygen molecule and the resulting O_2^- molecular ion plays the role of an anion. Then each O_2^- anion has nine electrons at the $2p$ molecular levels with the electronic configuration of $\sigma_g^2 \pi_u^4 \pi_g^3$ (see Fig. 1).² One hole in the antibonding ($2p$) π_g molecular state can generate the magnetic moment of $1 \mu_B$ for each O_2^- . Therefore these partially occupied antibonding ($2p$) π_g states in AO_2 superoxides are important in determining their electronic and magnetic properties, such as π -electron magnetism.³ At room temperature, KO_2 crystallizes in the

tetragonal [T] structure, in which the O_2^- molecular bond axes are parallel to the z axis (see Fig. 1).⁴ KO_2 retains this structure down to 197 K. Upon cooling, O_2^- molecular bond axes seem to tilt to have a lower crystal monoclinic symmetry. By lowering the crystal symmetry, the degeneracy of the π_g level is lifted, similarly as in the Jahn-Teller distortion.^{3,5}

Experimentally, however, the electronic structures of AO_2 superoxides have not been investigated much due to the difficulties in the sample preparation. KO_2 reacts violently with water, and may cause fire in contact with combustible material. In this work, we have studied the electronic structure of KO_2 by employing soft x-ray absorption spectroscopy (XAS) and core-level photoemission spectroscopy (PES), which are known to be powerful experimental tools for studying the electronic structures of solids.⁶⁻⁸ We have also compared the measured O $1s$ XAS spectrum with the calculated density of states (DOSs). For the electronic-structure calculations, we have used the full-potential augmented plane-wave band method⁹ implemented in the WIEN2K package.¹⁰ For the exchange-correlation potential, the generalized gradient approximation (GGA) (Ref. 11) was used. The on-site Coulomb interaction U between the oxygen $2p$ electrons (GGA + U) (Ref. 12) and the spin-orbit (SO) effect were included as a second variational procedure (GGA+SO+ U). The details of the calculation are described in Ref. 5.

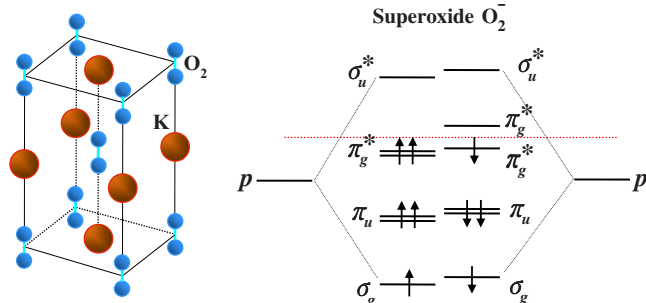


FIG. 1. (Color online) (Left) [T] structure of KO_2 . K atoms are denoted as red large spheres and O atoms are denoted as blue small spheres. (Right) Energy-level diagram for the superoxide O_2^- . Each O_2^- anion has nine electrons at the $2p$ molecular levels and the bonding σ_g and π_u states are completely filled while the antibonding π_g^* orbitals are partially filled. The red dotted line is added as a guideline to distinguish the unoccupied states from the occupied states.

II. EXPERIMENTAL DETAILS

PES and XAS experiments were performed at the 8A1 undulator beamline of the Pohang Light Source (PLS) at room temperature. The KO_2 sample used in this study was obtained in the powder form from Sigma-Aldrich Co., USA. After the seal of the sample bottle was opened, KO_2 sample had been kept in vacuum until it was measured at the PLS. Several samples were mounted on the sample holder by us-

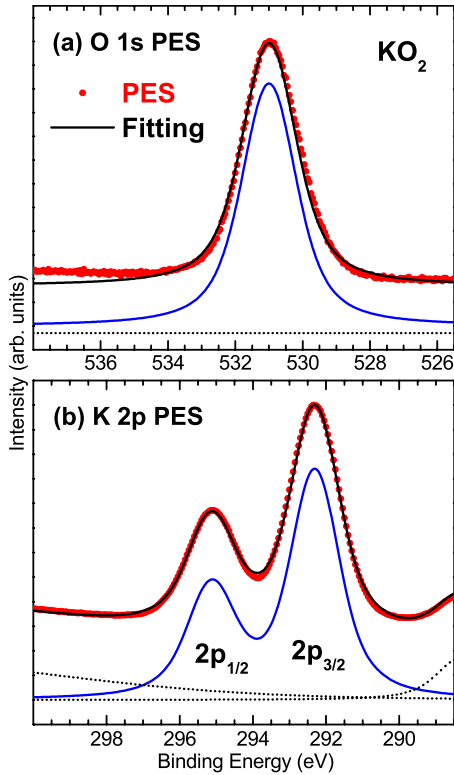


FIG. 2. (Color online) Core-level PES spectra of KO_2 along with the curve-fitting results for (a) the O $1s$ state and (b) the K $2p$ state, respectively. Solid dots represent the experimental data and solid lines are the curve-fitting results. See the text for the details.

ing a double-sided Cu tape or silver paste. After several trials and errors in the sample-mounting procedure to minimize the exposure time to the moisture in air, we were able to mount each KO_2 sample within less than a few minutes of the air-exposure time. As soon as the KO_2 sample was mounted on the holder, the holder was loaded in the load-lock chamber immediately, followed by pumping.

The base pressure of the XAS/PES chamber was better than 3×10^{-10} Torr. XAS spectra were obtained by employing the total electron yield mode with the photon energy resolution of ~ 100 meV at $h\nu \sim 500$ eV. The Fermi level E_F and the instrumental resolution of the system were determined from the valence-band spectrum of scraped Au in electrical contact with samples. The overall instrumental resolution of the PES spectra was about ~ 0.4 eV at $h\nu \sim 600$ eV. All the XAS and PES spectra were normalized to the incident photon flux. Only the potassium- (K-) and oxygen- (O-) related peaks were observed in the survey PES

spectra (not shown here), except for the existence of the carbon (C) $1s$ core level. A clean, single peak was observed in the O $1s$ core-level PES spectrum. These findings confirm that our PES/XAS data for KO_2 , presented in this work, are reliable.

III. RESULTS

Figure 2 provides the core-level PES spectra (red dots) of KO_2 , obtained with $h\nu = 650$ eV, along with the curve-fitting results (solid lines) for (a) the O $1s$ state and (b) the K $2p$ state, respectively. Note that the O $1s$ core-level PES spectrum of KO_2 exhibits a single and symmetric peak, indicating the good quality of our sample employed in this work. When we determine the binding energies (BEs) of PES spectra by using the sputtered Au metal in electrical contact with the KO_2 sample, the BE's of the O $1s$, K $2p_{3/2}$, and C $1s$ core levels in KO_2 become 537.6 eV, 298.9 eV, and 291.1 eV, respectively. This C $1s$ BE is too high. So we have instead used the C $1s$ core peak of KO_2 by setting it as 284.5 eV (Ref. 13) in the BE calibration of KO_2 spectra. Then the BE's of the O $1s$ and K $2p_{3/2}$ core-level peaks become 531.0 eV and 292.3 eV in KO_2 , respectively. The latter value is similar to that of KCl.¹³ These BE's are rather different from those in the literature for KO_2 film,^{14,15} which might be due to the difference between the *in situ* grown thin films and our *bulk* samples.

The measured core-level PES spectra were analyzed by using the Doniach-Sunjic line-shape function,¹⁶ as follows:

$$f(E) = \frac{\Gamma(1 - \alpha) \cos[\pi\alpha/2 + (1 - \alpha)\arctan(E/\gamma)]}{(E^2 + \gamma^2)^{(1-\alpha)/2}},$$

where E is the energy relative to the peak position, Γ denotes the gamma function, and 2γ corresponds to the full width at half maximum of the Lorentzian function. The intrinsic lifetime width is described by γ , which simulates the broadening due to a finite core-hole lifetime. The asymmetry parameter α accounts for the low-energy electron-hole excitations. Each peak is further convoluted with a Gaussian function to account for the broadening due to the instrumental resolution as well as that due to phonons. The background due to the inelastically scattered electrons is also added.

The parameter values determined from this fitting are listed in Table I. First, this fitting confirms that the O $1s$ core-level PES spectrum can be described by a single component. Similarly, the K $2p$ core-level PES spectrum of KO_2 is fitted well by using one α component only. Peak 1 and Peak 2 in K $2p$ states correspond to the $2p_{3/2}$ and $2p_{1/2}$ peak, re-

TABLE I. Fitting parameters employed in the O $1s$ and K $2p$ core-level PES spectra of KO_2 .

Core levels	BE (eV)		ΔE_{SO} (eV)	2γ (eV)	α	GB (eV)	Intensity I_2/I_1
	Peak 1	Peak 2					
O $1s$	531.0		0	1.1	0	1.2	
K $2p$	292.3	295.1	2.83	0.9	0	1.05	0.49

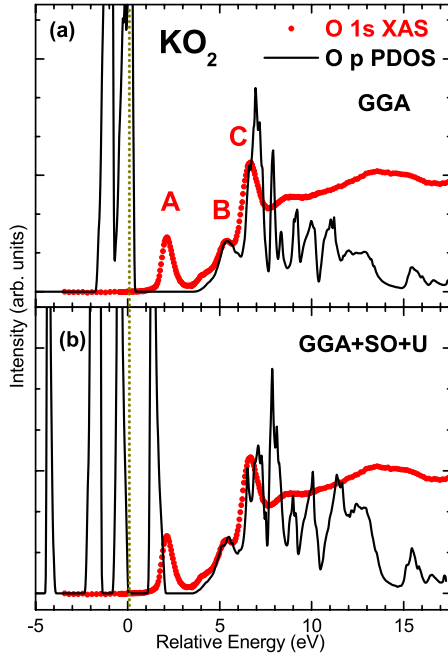


FIG. 3. (Color online) Comparison of the O $1s$ XAS spectrum of KO_2 with the calculated O $2p$ PDOS, which was obtained from (a) the GGA calculation, and from (b) the GGA+SO+ U calculation ($U=11.5$ eV), respectively. In both calculations, the FM phase of KO_2 with the $[T]$ structure was assumed.

spectively, with the SO splitting (ΔE_{SO}) of $\Delta E_{\text{SO}}=2.83$ eV. Therefore these core-level PES spectra confirm that our KO_2 sample is in the single phase and that our PES/XAS spectra represent the intrinsic features of KO_2 . Note that the Gaussian broadening (GB), employed in this fitting (GB ~ 1.05 – 1.2 eV), is much larger than the instrumental resolution (≈ 0.4 eV) of the present PES. Such large GB values seem to imply the large phonon effect in KO_2 , as is expected from the presence of the strong interplay among spin, orbital, and lattice degrees of freedom in degenerate π_g states.^{1,5}

Figure 3 compares the measured O $1s$ XAS spectrum of KO_2 (red dots) with the calculated DOS (solid lines). The O $1s$ XAS spectrum of KO_2 has been shifted by -526 eV and the peak positions are shown in the relative energy scale. Our O $1s$ XAS spectrum of KO_2 is similar to that of KO_2 film, which was prepared *in situ*^{15,17} but somewhat different from that of the later work by Pedio *et al.*¹⁸ The features in our XAS data are sharper than those in KO_2 films^{15,17,18} but the relative intensities are different. At the moment, we do not know the origin of such differences. However, the O $1s$ core-level PES spectrum for our sample exhibits a single clean peak, as shown in Fig. 2(a), and the quality of our O $1s$ XAS spectrum is much better than those of KO_2 films^{15,17,18} in both the signal-to-noise ratio and the instrumental resolution. Hence we consider our O $1s$ XAS spectrum to represent the intrinsic feature of KO_2 . One reason might be the difference between thin film samples^{15,17,18} and bulk samples (our data).

The calculated O $2p$ partial DOS (PDOS) in Fig. 3(a) was obtained from the GGA calculation, while that in Fig. 3(b) was obtained from the GGA+SO+ U calculation with U

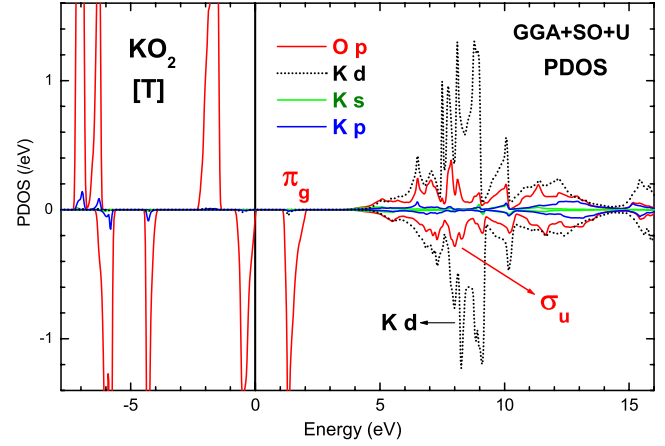


FIG. 4. (Color online) PDOS of O p , K s , p , d states for the FM phase of KO_2 with the $[T]$ structure, obtained from the GGA+SO+ U calculation ($U=11.5$ eV). The red solid line and black dotted line represent O p PDOS and K d PDOS, respectively.

$=11.5$ eV.¹⁹ In this figure the Fermi level (E_F) corresponds to $E=0$ eV. In both calculations, the ferromagnetic (FM) phase of KO_2 with the $[T]$ structure, shown in Fig. 1, was assumed since the O $1s$ XAS spectrum was obtained at room temperature. In the calculated PDOS, the lowest energy peak above E_F corresponds to the O $2p$ antibonding π_g states (see Figs. 1 and 4), and the high-energy peaks between 5 and 15 eV are dominated by the unoccupied PDOS of K s , p , and d states, but together with a contribution from the antibonding σ_u states of O $2p$ orbitals.⁵

Figure 3 shows that the energy separation between the lowest energy peak (A) and the higher energy peaks (B, C) in the O $1s$ XAS is quite different from that in the GGA calculation but agrees better with that in the GGA+SO+ U calculation. Note that both the sharp lowest energy peak (A: ~ 2 eV above E_F) and the higher energy double-peak structure (B and C: ~ 5 eV and ~ 7 eV above E_F) in the O $1s$ XAS agree well with those in the calculated PDOS. The improved agreement of GGA+SO+ U calculation with experiment in the energy separation comes from the increased splitting of $\pi_{g\downarrow}$ states (see Fig. 1) due to the combined effect of the spin-orbit and on-site Coulomb interactions. The energy separation between the unoccupied $\pi_{g\downarrow}$ and σ_u states (see Fig. 4) will decrease further by increasing U value in the calculation, which will then result in a better agreement with experiment. This finding indicates that it is important to include the SO interaction and the on-site Coulomb interaction U between O $2p$ electrons in the calculation of the electronic structure of KO_2 . In fact, this finding is consistent with that in the recent studies,^{1,5} which suggests the importance of the SO and U effects for the splitting of π_g states in KO_2 with the $[T]$ structure. The U effect of O $2p$ electrons was also examined for the similar $2p$ magnetic oxides, such as Rb_4O_6 and RbO_2 .^{20,21}

Figure 4 compares the calculated PDOS of O p , K s , p , and d states for the FM phase of KO_2 with the $[T]$ structure. These PDOS's are obtained from the same calculations, as shown in Fig. 3(b). In the GGA+SO+ U calculation, the O $2\pi_{g\downarrow}$ states are split into $\pi_{+1}(m=1)$ and $\pi_{-1}(m=-1)$,

which are located below and above E_F , respectively. The broad O p PDOS above E_F corresponds to the $O_2^- \sigma_u$ states (see Fig. 1). Note that the lineshape and the width of the $O_2^- \sigma_u$ PDOS are very similar to those of K s , p , and d PDOS's, indicating that the hybridization between $O_2^- \sigma_u$ and K s , p , and d states is large. This finding shows that the existing XAS analyses,^{17,18} which assume the sharp $O_2^- \sigma_u$ molecular levels for KO_2 , are not realistic. This figure also shows that the unoccupied K d states has a larger contribution to the spectral weight in 8–15 eV above E_F in the O $1s$ XAS spectrum than the unoccupied $O_2^- \sigma_u$ states.

IV. CONCLUSION

The electronic structure of superoxide KO_2 is investigated by employing XAS and core-level PES. We have compared the measured O $1s$ XAS spectrum with the calculated DOS, obtained from the GGA+SO+ U calculation. The measured

O $1s$ and K $2p$ core-level PES spectra of KO_2 are clean and only one symmetric component is observed in both of them. This observation confirms the good quality of the KO_2 sample employed in this work. Both the unoccupied O $2p$ antibonding π_g and σ_u states are observed in the O $1s$ XAS spectrum. It is found that the main features in the unoccupied states, observed in the O $1s$ XAS, agree reasonably well with the calculated DOSs, suggesting the importance of the SO effect and the on-site Coulomb interaction in KO_2 with the high-symmetry tetragonal structure.

ACKNOWLEDGMENTS

This work was supported by the NRF under Contracts No. 2009-0064246 and No. 2009-0079947. Y.H.J. acknowledges the NRF grant funded by the Korea government under Grant No. 2010-0014523. PLS is supported by POSTECH and MEST in Korea.

*Corresponding author; kangjs@catholic.ac.kr

- ¹I. V. Solovyev, *New J. Phys.* **10**, 013035 (2008), and references therein.
- ²J. J. Attema, G. A. de Wijs, and R. A. de Groot, *J. Phys.: Condens. Matter* **19**, 165203 (2007).
- ³M. A. Bösch, M. E. Lines, and M. Labhart, *Phys. Rev. Lett.* **45**, 140 (1980).
- ⁴W. Känzig and M. Labhart, *J. Phys. (Paris)* **37**, C7-39 (1976).
- ⁵M. Kim, B. H. Kim, H. C. Choi, and B. I. Min, *Phys. Rev. B* **81**, 100409(R) (2010).
- ⁶F. M. F. de Groot, J. C. Fuggle, B. T. Thole, and G. A. Sawatzky, *Phys. Rev. B* **42**, 5459 (1990).
- ⁷G. van der Laan and I. W. Kirkman, *J. Phys.: Condens. Matter* **4**, 4189 (1992).
- ⁸S. Hüfner, *Photoelectron Spectroscopy*, Solid-State Sciences Vol. 82 (Springer-Verlag, Berlin, 1995).
- ⁹M. Weinert, E. Wimmer, and A. J. Freeman, *Phys. Rev. B* **26**, 4571 (1982).
- ¹⁰P. Blaha, K. Schwarz, G. K. H. Madsen, D. Kvasnicka, and J. Luitz, *WIEN2k* (Technische Universität Wien, Austria, 2001).
- ¹¹J. P. Perdew, K. Burke, and M. Ernzerhof, *Phys. Rev. Lett.* **77**, 3865 (1996).
- ¹²V. I. Anisimov, I. V. Solovyev, M. A. Korotin, M. T. Czyzyk, and

- G. A. Sawatzky, *Phys. Rev. B* **48**, 16929 (1993).
- ¹³J. F. Moulder, W. F. Stickle, P. E. Sobol, and K. D. Bomben, *Handbook of X-Ray Photoelectron Spectroscopy* (Perkin-Elmer, Minnesota, 1992).
- ¹⁴M. C. Asensio, E. G. Michel, E. M. Oellig, and R. Miranda, *Appl. Phys. Lett.* **51**, 1714 (1987).
- ¹⁵C. Puglia, P. Bennich, J. Hasselström, P. A. Brühwiler, A. Nilsson, A. J. Maxwell, N. Martensson, and P. Rudolf, *Surf. Sci.* **383**, 149 (1997).
- ¹⁶S. Doniach and M. Sunjic, *J. Phys. C* **3**, 285 (1970).
- ¹⁷M. W. Ruckman, S. L. Jie Chen, Q. P. Kuiper, M. Strongin, and B. I. Dunlap, *Phys. Rev. Lett.* **67**, 2533 (1991).
- ¹⁸M. Pedio, Z. Y. Wu, M. Benfatto, A. Mascaraque, E. Michel, C. Ottaviani, C. Crotti, M. Peloi, M. Zacchigna, and C. Comincioli, *Phys. Rev. B* **66**, 144109 (2002).
- ¹⁹Such a large U value ($U=11.5$ eV) is not surprising and the corresponding U value in a molecular crystal will be much smaller due to screening. In fact, this U value is consistent with that used in Ref. 1, which corresponds to the intermolecular Coulomb interaction of ~ 3.6 eV.
- ²⁰J. Winterlik, G. H. Fecher, and C. Felser, *J. Am. Chem. Soc.* **129**, 6990 (2007).
- ²¹R. Kováčik and C. Ederer, *Phys. Rev. B* **80**, 140411(R) (2009).